Combustion Theory and Modelling
Publication details, including instructions for authors and subscription information:
http://www.tandfonline.com/loi/tctm20

Edge flames stabilized in a non-premixed microcombustor

Joanna A. Bieri [a] & Moshe Matalon [b]

[a] Mathematics and Computer Science , University of Redlands , Redlands, CA, 92373, USA

[b] Mechanical Science and Engineering , University of Illinois at Urbana-Champaign , Urbana, IL, 61801, USA

Published online: 27 Jul 2011.

To cite this article: Joanna A. Bieri & Moshe Matalon (2011) Edge flames stabilized in a non-premixed microcombustor, Combustion Theory and Modelling, 15:6, 911-932, DOI: 10.1080/13647830.2011.584634

To link to this article: http://dx.doi.org/10.1080/13647830.2011.584634

Combustion Theory and Modelling
Vol. 15, No. 6, 2011, 911–932

Edge flames stabilized in a non-premixed microcombustor

Joanna A. Bieri[a] and Moshe Matalon[b]

[a]*Mathematics and Computer Science, University of Redlands, Redlands, CA 92373, USA;*
[b]*Mechanical Science and Engineering, University of Illinois at Urbana-Champaign, Urbana, IL 61801, USA*

(*Received 2 January 2011; final version received 23 April 2011*)

The dynamics of an edge flame confined in a non-premixed microcombustor model is studied numerically within the context of a diffusive-thermal model. Fuel and oxidizer, separated upstream by a thin plate, flow through a channel with a prescribed velocity. At the tip of the plate, the fuel and oxidizer mix and, when ignited, an edge flame is sustained at some distance from the plate. The objective in this work is to consider the effects of confinement, differential diffusion, and heat loss on the dynamics of an edge flame in a narrow channel. We consider a wide range of channel widths and allow for changing Lewis numbers, and both adiabatic conditions and heat losses along the channel walls. The results illustrate how the flame shape and standoff distance are affected by the channel width, by mixture composition through variations in Lewis numbers and by heat losses. Conditions for flame stabilization, flame oscillations and flame extinction or blowoff are predicted.

Keywords: edge flame; flame oscillation; microcombustion; diffusion flame; heat loss

1. Introduction

There has been increasing interest in recent years in microscale combustion, because of its potential use as a heat source and in power generation. Consequently, there is a need to understand flame dynamics in confined regions of dimensions comparable to, or smaller than, the quenching distance. Several theoretical studies have considered the propagation of premixed flames in narrow channels and examined the effects of flow conditions, differential diffusion and heat loss to the channels walls [1–4], as well as specific issues concerned with sustaining combustion at the microscale, such as heat recirculation and catalytic reactions [5–10]. In contrast, combustion of non-premixed reactants in small scale burners, where the initially separated fuel and oxidizer streams are brought together, mixing and burning along a diffusion flame, has not been widely discussed. The advantage of the non-premixed configuration as opposed to a straight duct premixed combustor is that the mixing zone, and the resulting diffusion flame between the two streams, is likely to spread over the entire length of the reactor channel. Experimental observations [11–13], however, indicate that the flame dynamics is far more complex. Miesse *et al*. [11] studied methane–oxygen diffusion flames in a sub-millimeter microburner and observed a sequence of isolated reaction structures aligned with the direction of the gas flow, with the repetitive extinction–reignition events that depended on the inlet gas velocity and initial

*Corresponding author. Email: joanna_bieri@redlands.edu

ISSN: 1364-7830 print / 1741-3559 online

http://dx.doi.org/10.1080/13647830.2011.584634
http://www.tandfonline.com

mixture strength. In a subsequent paper [12] they examined the effect of variations in Lewis number on the flame structure, and argued that the appearance of "cells" along the channel is more likely caused by the inability of the mixture to overcome heat losses to the burner walls than due to a diffusive-thermal instability. Xu and Ju [13] have also observed the extinction–reignition flame pattern in a mesoscale combustor, and argued that heat losses to the channel walls play an important role in determining the length of the diffusion flame branches and the distance between successive "flamelets". These observations indicate that the burning characteristics in these non-premixed combustors are not well understood. Edge flames also play an important role in various engineering and fire safety applications, including lifted jet flames, flame spreading over liquid and solid beds and flames in mixing layers, where flame stabilization and onset of instabilities remain important research topics. A review of the experimental record was recently given by Chung [14].

The present work is concerned with combustion of non-premixed reactants in a narrow channel, a configuration that mimics the sub-millimeter microburner that was fabricated at the University of Illinois [11]. Two initially separated fuel and oxidizer streams flow into a narrow channel where combustion occurs. The flame often stands off the plate separating the two streams and stabilizes against the flow of the non-uniform partially premixed gas that forms as a result of the interdiffusion of the fuel and oxidizer. The resulting flame has a highly curved premixed edge, with lean and rich segments, and a diffusion flame trailing behind along the axis of the channel. Sustaining combustion in such a configuration depends primarily on the edge flame, its dynamics and stability.

Theoretical advances in the study of edge flames have been reviewed by Buckmaster [15] and Matalon [16]. There have been several numerical simulations, e.g., [17–20], that have examined the characteristics of the edge of the flame as part of the overall flame structure. The most relevant studies to the present investigation are those of Kurdyumov and Matalon [21–24] who focused on edge flames in mixing layers. Using a diffusive-thermal model with a prescribed uniform flow, they considered the influence of differential diffusion, mixture strength, flow rate, and heat loss on edge flame dynamics [21, 22]. They determined conditions for flame stabilization and showed that when the flow rate is sufficiently high and/or when radiative losses are appreciable, spontaneous oscillations occur with the flame moving back and forth, unable to stabilize at the expected location. Oscillations typically occur when one of the two Lewis numbers, associated with either the fuel or the oxidizer, is larger than unity and when the fuel and oxidizer are supplied at conditions remote from stoichiometry. In order to determine the influence of the flow field in the mixing layer on combustion they reexamined the problem using the non-uniform flow computed from the full Navier–Stokes equations [23] and confirmed the earlier predictions concerning the conditions for flame stabilization and onset of oscillations. More recently, they investigated the effects of thermal expansion, extending their previous model to allow for density changes due to the heat released by the flame [24]. The primary effect of thermal expansion was found to be the relocation of the edge flame closer to the splitter plate. Flame oscillations were predicted under similar conditions to the previous studies implying that oscillations, associated with a diffusive-thermal instability, may be qualitatively predicted by a diffusive-thermal model and are not a result of the simplifying constant-density assumption. In all of these studies combustion occurs in an unconfined mixing layer. In contrast, the present work examines the effects of confinement by considering the edge flame in a narrow channel. The effect of gas expansion on an edge flame stabilized in a channel has been recently discussed by Bieri *et al*. [25]. Here the focus is on the flame dynamics and stability.

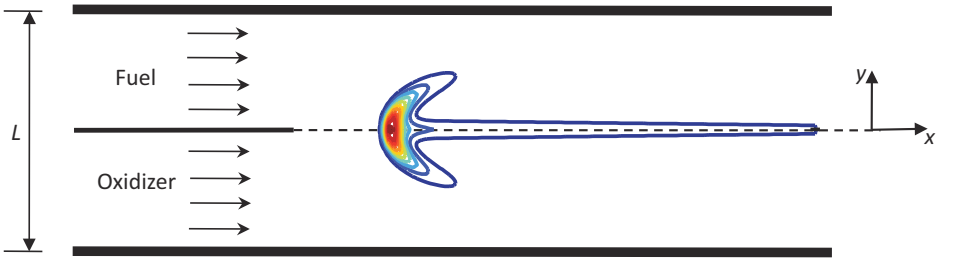

Figure 1. A schematic of an edge flame stabilized in a narrow channel.

2. Formulation

Consider a semi-infinite plate that separates two parallel streams, one containing fuel with mass fraction $Y_{F_{-\infty}}$, and the other oxidizer with mass fraction $Y_{O_{-\infty}}$, that flow into a narrow channel of width L at a uniform constant velocity U (see Figure 1). The plate is assumed to have high enough thermal conductivity so that its temperature remains constant and equal to the temperature $T_{-\infty}$ of the two incoming streams. Beyond the tip of the separating plate the fuel and oxidizer mix, and when ignition is successful a flame is sustained at some distance from the tip of the plate. Typically, the edge of the flame has a tribrachial structure as shown in the figure; it consists of a fuel-rich branch extending toward the fuel side and a fuel-lean branch extending toward the oxidizer side, with the diffusion flame trailing behind. The chemical reaction is described by a one step, irreversible reaction of the form

$$\text{Fuel} + \nu\,\text{Oxidizer} \rightarrow (1+\nu)\text{Product} \tag{1}$$

where ν is the mass-weighted oxidizer-to-fuel stoichiometric ratio. Conductive heat loss at the channel walls, modeled by Newton's law with an appropriately defined heat transfer number K, is given by $K(\tilde{T} - T_{-\infty})$, where $\tilde{T}$ is the temperature of the gas mixture adjacent to the walls.

We adopt a diffusive thermal model, such that the density of the mixture ρ, the heat capacity c_p, the thermal diffusivity $\mathcal{D}_{\text{th}} \equiv \lambda/\rho c_p$ with λ the thermal conductivity, and the individual molecular diffusivities $\mathcal{D}_F$ and $\mathcal{D}_O$ are all assumed constant. The governing equations then reduce to balance equations for the individual mass fractions $\tilde{Y}_F$, $\tilde{Y}_O$ and an energy equation for the whole mixture, expressed in terms of the temperature $\tilde{T}$. The imposed, underlying velocity U is chosen as a unit of speed, the diffusion length $l_{\text{th}} \equiv \mathcal{D}_{\text{th}}/U$ as a unit of length, and the diffusion time $\mathcal{D}_{\text{th}}/U^2$ as a unit of time. Consequently, the channel width in dimensionless form is denoted by $h = L/l_{\text{th}}$. The mass fractions are normalized with respect to their values in the supply streams such that $Y_F = \tilde{Y}_F/Y_{F_{-\infty}}$ and $Y_O = \tilde{Y}_O/Y_{O_{-\infty}}$, and a non-dimensional temperature is defined by $\theta = (\tilde{T} - T_{-\infty})/(T_s - T_{-\infty})$. Here T_s is the stoichiometric temperature corresponding to complete reactant consumption, given by

$$T_s = T_{-\infty} + \frac{QY_{F_{-\infty}}}{c_p(1+\phi)} \tag{2}$$

where Q is the total heat release and $\phi = \nu Y_{F_{-\infty}}/Y_{O_{-\infty}}$ represents the initial mixture strength. (The notation adopted in the paper is such that when the same symbol is used, the one with the ˜ represents the dimensional quantity.)

In dimensionless form, the governing equations are

$$\frac{\partial Y_F}{\partial t} + \frac{\partial Y_F}{\partial x} - Le_F^{-1}\left(\frac{\partial^2 Y_F}{\partial x^2} + \frac{\partial^2 Y_F}{\partial y^2}\right) = -D\,\omega \tag{3}$$

$$\frac{\partial Y_O}{\partial t} + \frac{\partial Y_O}{\partial x} - Le_O^{-1}\left(\frac{\partial^2 Y_O}{\partial x^2} + \frac{\partial^2 Y_O}{\partial y^2}\right) = -\phi D\,\omega \tag{4}$$

$$\frac{\partial \theta}{\partial t} + \frac{\partial \theta}{\partial x} - \left(\frac{\partial^2 \theta}{\partial x^2} + \frac{\partial^2 \theta}{\partial y^2}\right) = (1+\phi)D\,\omega \tag{5}$$

with

$$\omega = \beta^3 Y_F Y_O \exp\left[\frac{\beta(\theta-1)}{(1+\gamma\theta)/(1+\gamma)}\right]. \tag{6}$$

These must be solved subject to the following boundary conditions:
far upstream as $x \to -\infty$:

$$\theta = 0\,, \qquad \begin{array}{ll} Y_F = 1,\ Y_O = 0 & y > 0 \\ Y_F = 0,\ Y_O = 1 & y < 0\,, \end{array} \tag{7}$$

along the separating plate $y = 0\,,\ -\infty < x < 0$:

$$\theta = 0\,, \qquad \partial Y_F/\partial y\big|_{y=0^+} = \partial Y_O/\partial y\big|_{y=0^-} = 0\,, \tag{8}$$

at the channel walls $y = \pm h/2$:

$$\partial Y_F/\partial y = \partial Y_O/\partial y = 0\,, \qquad -\partial\theta/\partial y = \pm k\theta\,. \tag{9}$$

The parameters appearing in these equations are: the Zel'dovich number $\beta = E(T_s - T_{-\infty})/R^0 T_s^2$, with E the activation energy and R^0 the gas constant, the Damköhler number

$$D = \beta^{-3}(\rho\mathcal{D}_{\rm th}/U^2)\mathcal{B}Y_{O_{-\infty}}\,\mathrm{e}^{-E/R^0 T_s}\,,$$

with $\mathcal{B}$ the pre-exponential factor of the chemical reaction rate, the heat release parameter $\gamma = (T_s - T_{-\infty})/T_{-\infty}$, the Lewis numbers $Le_F = \mathcal{D}_{\rm th}/\mathcal{D}_F$ and $Le_O = \mathcal{D}_{\rm th}/\mathcal{D}_O$ for the fuel and oxidizer, respectively, and the heat transfer parameter $k = K/\rho c_p U$.

We note that the premixed flame segment forming the curved edge of the flame is characterized by the laminar flame speed $S_{\rm L}$, which implies that the Damköhler number $D \sim S_{\rm L}^2/U^2$. The quenching distance, on the order of the laminar flame thickness, is typically $\sim 5l_{\rm th}$, so that narrow channels with $h \leq 5$ are, indeed, in the sub-millimeter range. We also note that $h = RePr$ where Re is the Reynolds number based on the channel's width and Pr is the Prandtl number. Thus, for the channel widths considered, the Reynolds number is on the order of 1 to 10.

Equations (3)–(5) were solved numerically using a second order, finite difference approximation in space. Both steady and time-dependent calculations were performed. The time-dependent equations were solved using an explicit marching procedure in order to determine *stable* steady states, when the solution converges to a time-independent state, and *stable* oscillatory states, when the solution evolves into a bounded but time-dependent state. To determine all the possible steady states, including unstable ones, solutions of the steady equations were sought. For such calculations an iterative procedure was used in which the same unsteady equations were solved but with the additional constraint that the temperature at a judiciously chosen reference point in the computational domain (x^*, y^*) is prescribed, namely $\theta(x^*, y^*) = \theta^*$. Typically the temperature was forced along the center of the channel with $\theta^* \approx 0.60$ and $0 \leq x^* \leq 15$. This additional condition allows us to iterate on one of the other parameters, e.g., the Damköhler number, until the solution has converged to within some acceptable error; in most cases this was taken to be on the order of 10^{-8}. Time in this approach has only an iterative role with no physical meaning attached to the transient states. In all cases the calculations were performed on a finite domain with a rectangular uniform grid typically 200 points in each direction. The independence of the solution to this choice was confirmed.

Steady solutions were found first and the results displayed as a function of one of the parameters. This allows the determination of response curves that exhibit the dependence of all possible solutions (stable and unstable) in terms of the parameters. The unsteady code was then used to test the stability of the steady states. To test the steady states for stability we examine the evolution in time starting from some arbitrary initial conditions. Typically, the initial conditions were chosen to correspond to a slightly disturbed steady solution. If a steady state reemerges as the long-time behavior of the initial value problem, the corresponding steady state solution is considered stable. If the steady state is unstable the time-dependent solution may converge to a new bounded oscillatory state, or diverge in time. The latter is of no physical interest.

In this work we choose $\phi = 1$, and assume $Le_F = Le_O \equiv Le$, so that our results are limited to symmetric flames. The position of the edge flame may be defined in general as the location where the reaction rate reaches its maximum value, namely (x_w, y_w) where $\omega = \omega_{max}$. For symmetric flames $y_w = 0$ and the location is solely determined by $x = x_w$. For unequal Lewis numbers and/or non-unity values of ϕ the edge moves away from the centerline and the entire flame leans to one or the other side of the axis. The adopted choice was primarily made for simplicity, since the non-symmetric flame behavior adds a complexity that sidetracks the main objective of this study. Future work will consider effects due to preferential diffusion $Le_F \neq Le_O$ and stoichiometry $\phi \neq 1$. It should be noted, however, that these parameters can be controlled in an experiment by diluting the fuel and/or oxidizer with an appropriate inert.

For the calculations presented in this paper, the heat release parameter and the Zel'dovich number were assigned the values $\gamma = 5$ and $\beta = 10$, which are typical for hydrocarbon–air flames [26].

It is instructive to define the *overall burning rate* under steady conditions as the total mass of reactants consumed per unit time, namely

$$\Omega \equiv \frac{2D}{h} \int_{-h/2}^{h/2} \int_{-\infty}^{\infty} \omega \, dx dy \, .$$

Integrating Equations (3) and (4) throughout the entire channel and using the appropriate boundary conditions yields $\Omega = 1 - (Y_{F_\infty} + Y_{O_\infty})$, where Y_{O_∞} and Y_{F_∞} are the values of

the mass fractions far downstream. Since for finite values of β the reaction rate does not vanish identically no matter how small the temperature is, the chemical reaction in a sufficiently long channel will proceed until all the fuel and oxidizer are completely consumed. Most of the reactants are typically consumed along the curved premixed edge flame, and the excess that leaks through burns along the trailing diffusion flame. Indeed, under adiabatic conditions, the temperature of the combustion products remains near the stoichiometric temperature T_s and all the available reactants are consumed in the channel, so that $Y_{F_\infty} = Y_{O_\infty} = 0$ as $x \to \infty$ and $\Omega = 1$. For realistic values of β, however, the reaction rate is exponentially small when the temperature is reduced slightly below T_s. In the presence of heat loss the temperature near the walls drops significantly, the reaction rate becomes extremely small and practically negligible. For $\theta \approx 0.2$, for example, the reaction rate for $\beta = 10$ is on the order of 10^{-10}. With the reaction effectively frozen, one may expect residual fuel and/or oxidizer far downstream with an overall burning rate $\Omega < 1$.

The discussion in the next section starts with two limiting cases where the equations reduce significantly and provide results that, as we shall see, are consistent with the complete numerical solution. Our numerical results begin by considering adiabatic walls and systematically examine the effect of confinement on the edge flame location, structure and stability for channel widths ranging from wide channels, $h = 20$, to narrow channels on the order of the quenching distance, $h = 3$. The effect of differential diffusion on confined adiabatic flames is examined next. Finally, we discuss the effect of heat losses on the stand-off distance, structure and stability, allowing k to range from the adiabatic limit, $k = 0$, to sufficiently large values that correspond to cold isothermal walls.

3. Results and discussion

Before presenting the numerical results we examine two limiting cases: (i) the fast chemistry limit $D \to \infty$, and (ii) very narrow channels $h \to 0$.

3.1. *Fast chemistry limit*

In the limit $D \to \infty$ the reaction time is much faster than the diffusion time and combustion, restricted to the immediate vicinity of the channel's axis, is described on the scaled time $\tau = D\,t$ and coordinates $\hat{x} = D^{1/2}x$ and $\hat{y} = D^{1/2}y$. To leading order, the governing equations (after setting $\phi = 1$ and adopting a single Lewis number) become

$$\frac{\partial Y_F}{\partial \tau} - Le^{-1}\left(\frac{\partial^2 Y_F}{\partial \hat{x}^2} + \frac{\partial^2 Y_F}{\partial \hat{y}^2}\right) = -\omega \tag{10}$$

$$\frac{\partial Y_O}{\partial \tau} - Le^{-1}\left(\frac{\partial^2 Y_O}{\partial \hat{x}^2} + \frac{\partial^2 Y_O}{\partial \hat{y}^2}\right) = -\omega \tag{11}$$

$$\frac{\partial \theta}{\partial \tau} - \left(\frac{\partial^2 \theta}{\partial \hat{x}^2} + \frac{\partial^2 \theta}{\partial \hat{y}^2}\right) = 2\omega\,. \tag{12}$$

The upstream boundary conditions and the conditions along the separating plate remain unchanged if x, y are replaced with $\hat{x}$, $\hat{y}$, while the conditions at the walls are replaced by $\partial Y_F/\partial \hat{y} = \partial Y_O/\partial \hat{y} = \partial \theta/\partial \hat{y} = 0$ as $\hat{y} \pm \infty$. The solution in this limit can be obtained

numerically as a special case of the general equations (3)–(5) by neglecting convection, setting $D = 1$, $k = 0$ and $h \to \infty$. With combustion limited to the center of the channel, convection and, similarly, heat losses are evidently secondary effects. The long time behavior of the solution, starting with arbitrary initial conditions, is a stable flame sheet that extends along the axis of the channel and separates the region $y > 0$ where there is fuel but no oxidizer from the region $y < 0$ where there is only oxidizer. The unconditional stability of the flame in this limit was established by Kurdyumov and Matalon [22]. The edge position $\hat{x}_w = C$ is obtained by solving the steady problem (10)–(12), and may be expressed as

$$x_w = C D^{-1/2}. \tag{13}$$

For $Le = 1.7$, for example, we find that $C = 31.62$, a result shown in Figure 2 by the dashed curve.

We conclude that for large values of D, corresponding to a sufficiently low speed U_0, the flame is stabilized near the tip of the plate separating the two streams, and the standoff distance increases with decreasing D according to (13).

3.2. *Very narrow channels*

To examine the case of a very narrow channel, $h \ll 1$, we introduce the scaled coordinate $\eta = y/h$, which is equivalent to using the channel width as a unit for vertical length while retaining l_{th} as a unit for axial length. Introducing this scaling, the time-independent

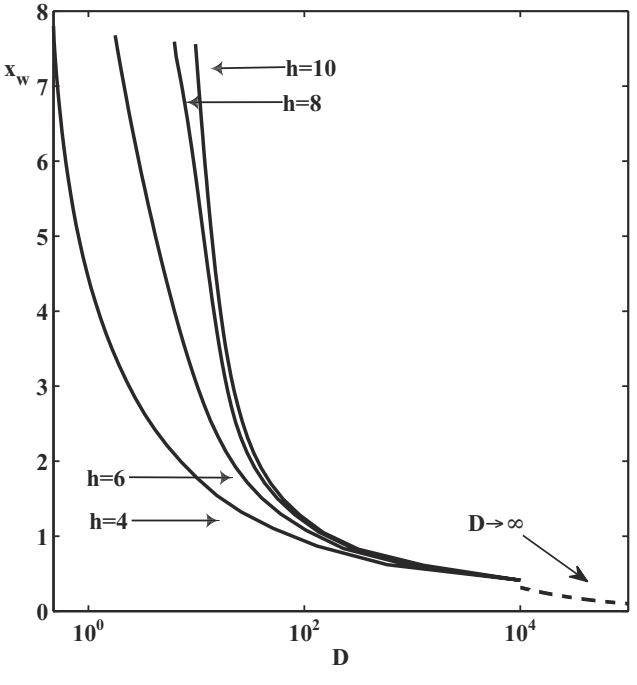

Figure 2. Flame standoff distance x_w as a function of the Damköhler number D, calculated for $k = 0$, $Le = 1.7$ and $\phi = 1$.

governing equations become

$$\frac{\partial Y_F}{\partial x} - Le^{-1}\left(\frac{\partial^2 Y_F}{\partial x^2} + \frac{1}{h^2}\frac{\partial^2 Y_F}{\partial \eta^2}\right) = -D\omega$$
$$\frac{\partial Y_O}{\partial x} - Le^{-1}\left(\frac{\partial^2 Y_O}{\partial x^2} + \frac{1}{h^2}\frac{\partial^2 Y_O}{\partial \eta^2}\right) = -D\omega$$
$$\frac{\partial \theta}{\partial x} - \left(\frac{\partial^2 \theta}{\partial x^2} + \frac{1}{h^2}\frac{\partial^2 \theta}{\partial \eta^2}\right) = 2D\omega\,.$$

The boundary conditions (7)–(9) remain the same after replacing y with η except for the heat flux condition at the walls $\eta = \pm 1/2$, which now reads $-\partial\theta/\partial\eta = \pm h\,k\,\theta$. We note, however, upon integrating the energy equation (5) throughout the entire channel and using the boundary conditions, that

$$\Omega = \frac{k}{h}\int_{-\infty}^{\infty} [\theta(x, 1/2) + \theta(x, -1/2)]\,dx\,,$$

implying that $k = O(h)$. We thus introduce $\hat{k} = k/h = O(1)$ and rewrite the conditions at $\eta = \pm 1/2$ as $-\partial\theta/\partial\eta = \pm h^2\,\hat{k}\,\theta$.

To leading order, the governing equations and boundary conditions simplify to

$$\partial^2 Y_F/\partial\eta^2 = \partial^2 Y_O/\partial\eta^2 = \partial^2\theta/\partial\eta^2 \sim 0$$
$$\partial Y_F/\partial\eta = \partial Y_O/\partial\eta = \partial\theta/\partial\eta = 0 \qquad \text{at } \eta = \pm 1/2\,,$$

which imply that all three variables are independent of η. The solution may therefore be expressed in the form

$$Y_F(x,\eta) = \overline{Y_F}(x) + h^2 Y_{F_1}(x,\eta) + \cdots$$
$$Y_O(x,\eta) = \overline{Y_O}(x) + h^2 Y_{O_1}(x,\eta) + \cdots$$
$$\theta(x,\eta) = \overline{\theta}(x) + h^2\theta_1(x,\eta) + \cdots\,,$$

with the second order terms satisfying

$$Le^{-1}\frac{\partial^2 Y_{F_1}}{\partial\eta^2} = \frac{d\overline{Y_F}}{dx} - Le^{-1}\frac{d^2\overline{Y_F}}{dx^2} + D\,\bar{\omega}$$
$$Le^{-1}\frac{\partial^2 Y_{O_1}}{\partial\eta^2} = \frac{d\overline{Y_O}}{\partial x} - Le_O^{-1}\frac{d^2\overline{Y_O}}{dx^2} + D\,\overline{\omega}$$
$$\frac{\partial^2\theta_1}{\partial\eta^2} = \frac{d\overline{\theta}}{dx} - \frac{d^2\overline{\theta}}{dx^2} - 2D\,\overline{\omega}$$

where $\overline{\omega} = \omega(\overline{Y_F}, \overline{Y_O}, \overline{\theta})$. At the walls, $\eta = \pm 1/2$, the boundary conditions simplify to $-\partial\theta_1/\partial\eta = \pm\hat{k}\bar{\theta}$ and $\partial Y_{F_1}/\partial\eta = \partial Y_{O_1}/\partial\eta = 0$. Integrating with respect to η, then applying

the boundary conditions at $\eta = \pm 1/2$, yields

$$\frac{d\overline{Y_F}}{dx} - Le^{-1}\frac{d^2\overline{Y_F}}{dx^2} = -D\,\overline{\omega} \tag{14}$$

$$\frac{d\overline{Y_O}}{dx} - Le^{-1}\frac{d^2\overline{Y_O}}{dx^2} = -D\,\overline{\omega} \tag{15}$$

$$\frac{d\overline{\theta}}{dx} - \frac{d^2\overline{\theta}}{dx^2} = 2D\,\overline{\omega} - 2\hat{k}\overline{\theta}\,. \tag{16}$$

This approximation, however, fails in the immediate vicinity of the tip of the plate so that the upstream boundary conditions cannot be imposed directly on $\overline{\theta}$, $\overline{Y_F}$ and $\overline{Y_O}$. Instead, a matching condition must be derived from the local solution near the tip of the plate, a region of axial dimension on the order $O(h)$.

The solution near the tip of the plate is obtained by rescaling the x-coordinate, writing $\xi = x/h$. To leading order, the problem reduces to

$$\nabla^2 Y_F = \nabla^2 Y_O = \nabla^2\theta \sim 0\,; \qquad \nabla^2 \equiv \frac{\partial^2}{\partial\xi^2} + \frac{\partial^2}{\partial\eta^2} \tag{17}$$

which must be solved with the same conditions at $\eta = \pm 1/2$ as above, and the upstream requirements $\theta = Y_O = 0$, $Y_F = 1$ for $\eta > 0$ and $\theta = Y_F = 0$, $Y_O = 1$ for $\eta < 0$, as $\xi \to -\infty$. Clearly $\theta(\xi, \eta) \equiv 0$, and the solutions for Y_F and Y_O represent the result of mixing that takes place as the fuel and oxidizer interdiffuse into each other. Representative profiles of the fuel mass fraction Y_F as a function of η at different stations ξ are shown in Figure 3; similar profiles can be obtained for the oxidizer mass fraction Y_O. The matching condition can be easily obtained by integrating Equations (17) across the entire volume $-\infty < \xi, \eta < \infty$, making use of the boundary conditions. One finds $Y_F = Y_O \sim 1/2$ as $\xi \to \infty$, consistent with the result shown in Figure 3. The matching conditions to be imposed on the solution

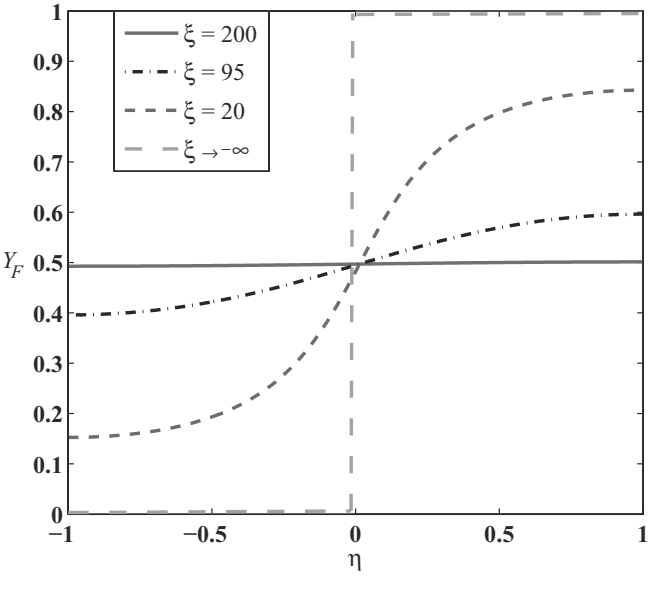

Figure 3. Fuel mass fraction profiles in the mixing region near the tip of the splitter plate.

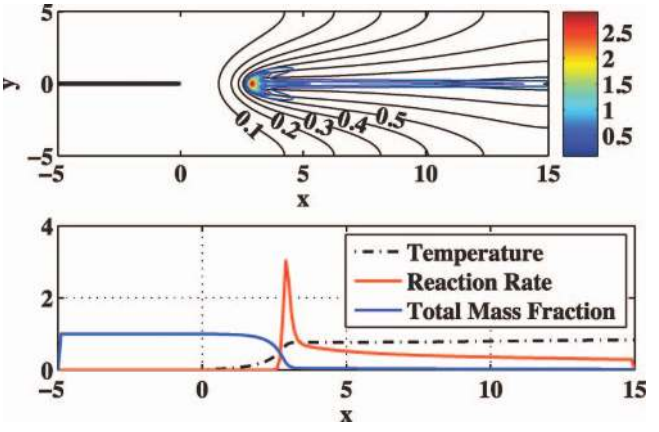

Figure 4. Edge flame in a channel of moderate width $h = 10$ and adiabatic walls. Top: reaction rate contours (in color) showing the tribrachial structure of the edge flame and temperature contours (in black). Bottom: reaction rate, temperature, and total mass fraction profiles along the axis $y = 0$. Calculated for $k = 0$, $D = 22$, $Le = 1.7$ and $\phi = 1$.

of Equations (14)–(16) are therefore $\overline{\theta} = 0$, $\overline{Y_F} = \overline{Y_O} = 1/2$, as $x \to 0$, implying that the fuel and oxidizer are well-mixed.

For very narrow channels, $h \ll 1$, the problem is thus identical to the classical problem of a one-dimensional premixed flame in the presence of volumetric heat loss of intensity $\hat{k}$, which mimics the conductive losses at the walls and is inversely proportional to the channel's width. This one-dimensional problem has well known analytical solutions under the assumption of a large activation energy parameter [27]. When adapted to the present setup, solutions are in the form of planar flames sustained at a distance inversely proportional

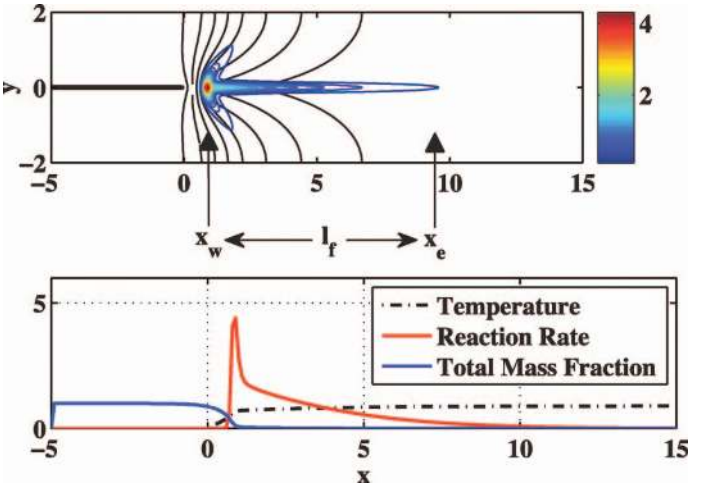

Figure 5. Edge flame in a narrow channel of width $h = 4$ and adiabatic walls. Top: reaction rate contours (in color) showing the tribrachial structure of the edge flame and temperature contours (in black). Bottom: reaction rate, temperature, and total mass fraction profiles along the axis $y = 0$. Calculated for $k = 0$, $D = 130$, $Le = 1.7$ and $\phi = 1$.

to D, with steady burning occurring for $\hat{k} < \hat{k}_{\text{ext}}$ only. The flame is extinguished when the intensity of the losses is substantial. This suggests that in very narrow channels the fuel and oxidizer mix well and burn along a nearly planar front provided that heat losses to the walls are not too excessive. The flame behaves like a premixed flame whose standoff distance is commensurate with the propagation speed, via $D \sim S_{\text{L}}^2/U^2$. As the channel becomes wider, the dead space near the walls where heat losses overcome the chemical reaction rate widens and the flame wings curve downstream; further discussion on the effect of heat loss on channels of various width can be found in [2]. One-dimensional models accounting for radiative losses or heat exchange between adjacent flames in multiple channels were reported in [28, 29].

3.3. *Adiabatic flames*

Next we consider numerical solutions for the case of adiabatic walls ($k=0$) and take $Le=1.7$, a choice motivated by the fact that the flame in an unconfined mixing layer for such Lewis numbers exhibits both stable and oscillating states. For sufficiently wide channels, e.g., $h=20$, we recover the results of Kurdyumov and Matalon [22] of an edge flame in an unconfined mixing layer. For moderately wide channels, $h=10$, the edge flame retains the typical tribrachial shape and burning persists along the trailing diffusion flame that extends to the end of the computational domain, as shown in Figure 4. Representative reaction rate contours (in color), ranging from $\omega = 0.1$, in steps of 0.1 between contours, up to $\omega_{\max}$, and isotherms $0.1 \leq \theta \leq 1$ in steps of 0.1 between contours (black curves) are shown in the top figure. Profiles of the temperature θ, reaction rate ω and the mass fraction of the total reactants $(Y_F + Y_O)$ along the axis are plotted in the bottom figure. The temperature increases through the premixed flame, where the reaction rate reaches its maximum, then varies slightly along the diffusion flame and tends to T_s as $x \to \infty$.

Similar results corresponding to a narrower channel, $h = 4$, are shown in Figure 5. Although the flame retains its tribrachial structure, the burning along the diffusion flame is limited to a finite distance from the leading edge. The location where the reaction rate vanishes, here taken as $\omega = 0.1$, may be used to identify the trailing edge x_{e}, and define a "flame length" $l_{\text{f}} = x_{\text{e}} - x_{\text{w}}$ (since for the symmetric flames under consideration the diffusion flame is aligned with the y-axis) as shown in the figure.

For all values of h, the edge flame is stabilized closer the tip of the plate for low flow rates (large values of D) and at increasingly larger distances as the flow rate increases (i.e., D decreases). This is shown in Figure 2 where the flame standoff distance, x_{w}, is plotted as a function of Damköhler number, inversely proportional to U^2, for varying channel widths. For large D, all curves tend to the asymptotic relation (13), also shown in the figure by a dashed curve. For sufficiently high velocities the flame is blown off the channel (i.e., the computational domain). For narrower channels, the flame can be stabilized for significantly higher values of the gas velocity, or smaller values of the Damköhler number. For a given flow rate, corresponding to $D = 1$ say, an edge flame can be stabilized in a channel with width $h = 4$ at a distance $x_{\text{w}} = 4.5$ from the tip of the plate. But the same flame will be blown off by the relatively high flow rate in channels of width $h = 6$ and larger. Stabilization at these high flow rates in narrow channels is due to the lateral confinement, which enhances the fuel and oxidizer mixing ahead of the premixed flame segment.

In Figure 6 the flame structure is shown in two channels of different widths, for the same flow rate corresponding to $D = 10$. In the wide channel the flame stands at a significantly

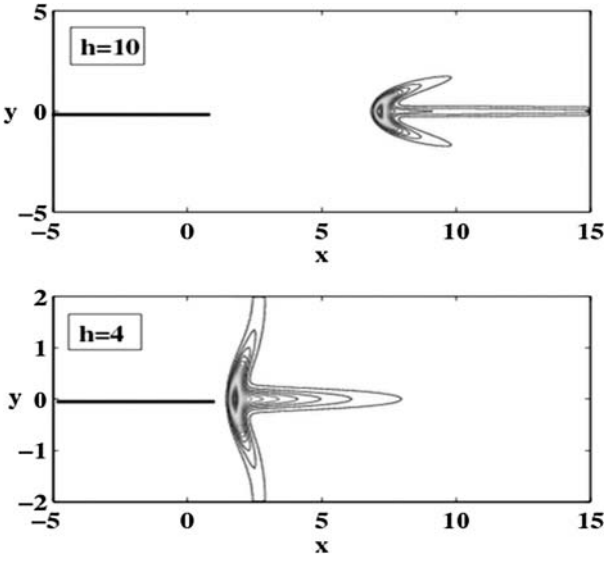

Figure 6. Comparison of the flame structure in two channels of different width and for the same flow rate corresponding to $D = 10$. Calculated for $k = 0$, $Le = 1.7$ and $\phi = 1$.

larger distance from the tip of the separating plate ($x_w \approx 7$) and has a highly curved premixed edge with lean and rich segments extending downstream. When the width of the channel is decreased relative to the diffusion length, a greater fraction of the flow is forced into the diffusion zone, which increases the overall level of fuel and oxidizer mixing ahead of the flame. As a result the weakly curved premixed flame segment extends almost throughout the entire channel width. The standoff distance is shorter ($x_w \approx 1.8$) and the flame is of finite extent, with $l_f \approx 5$, i.e., on the order of the channel width.

In Figure 7 we show the effect of varying the flow rate in a narrow channel of width $h = 4$. Some reminiscence to the tribrachial structure can be seen for $D = 2.7$. The flame

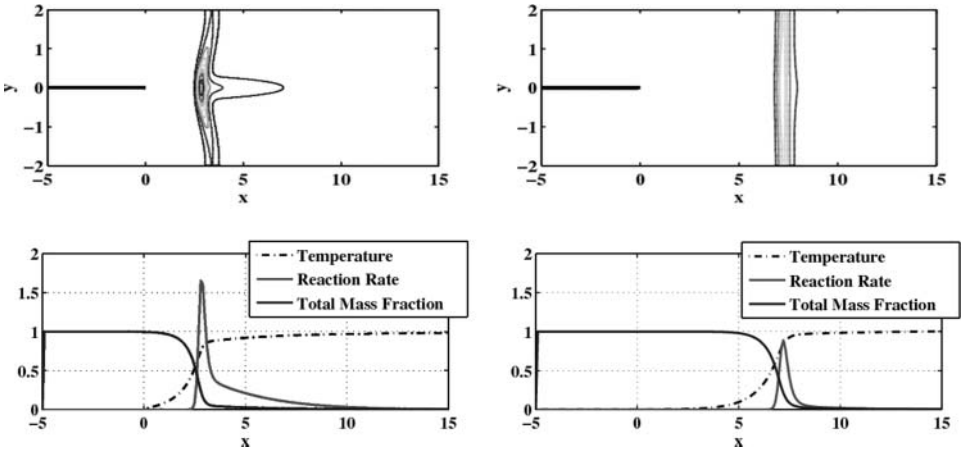

Figure 7. Comparison of the flame structure in two channels of the same width for increasing flow rates. Top: reaction rate contours; bottom: reaction rate, temperature, and total mass fraction profiles along the axis $y = 0$. Calculated for $k = 0$, $Le = 1.7$ and $\phi = 1$.

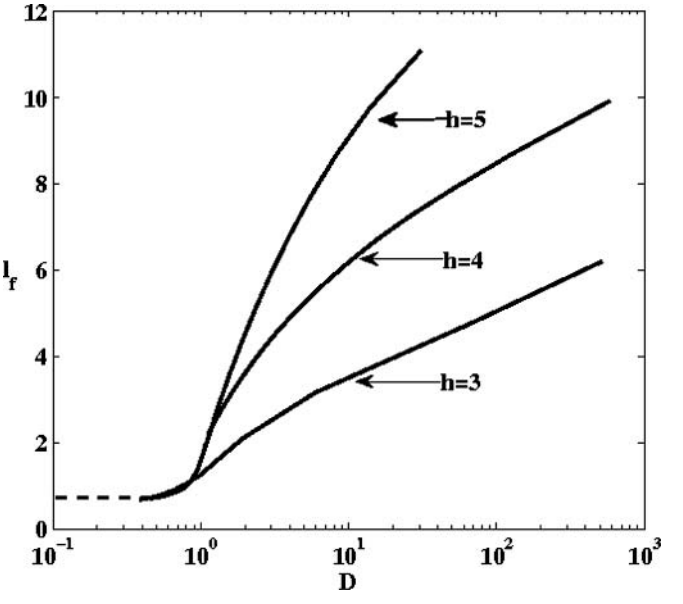

Figure 8. Flame length in narrow channels as a function of the Damköhler number; the dashed line represents the planar premixed flame thickness.

is nearly planar, but of weakly varying strength along its front. The leakage of reactants is small, so that the resulting diffusion flame is limited to a very small region behind the premixed flame front. The remaining reactants are consumed immediately behind the premixed front and the trailing diffusion flame ends at a finite location. For $D = 0.5$ the strength of the reaction is no longer focused at the center of the channel, but is spread across the entire width of the channel, and the flame is practically a planar premixed flame, with the temperature reaching the stoichiometric flame temperature $\theta = 1$. This result is consistent with the asymptotic approximation obtained for $h \ll 1$, discussed previously.

In Figure 8 we show the flame length l_f as a function of Damköhler number for three values of the channel width. Indeed, l_f decreases with increasing flow rate (decreasing D) and tends to a constant, approximately equal to the thickness of a planar adiabatic premixed flame, used in this study as unit of length, when $D \to 0$.

An important conclusion drawn from the earlier studies of edge flames in unconfined mixing layers [22] is the development of flame instabilities in the form of spontaneous oscillations. These were found to occur for sufficiently large values of the Lewis number, similar to the one considered here, and at high flow rates when D is reduced to below a critical value D^*. It was found that for $D > D^*$ the flame, after an initial transient, tends back to its steady position and retains this value thereafter. In contrast, for $D < D^*$ spontaneous oscillations develop with the edge of the flame moving back and forth about the steady state position. In the unconfined case, for $Le = 1.7$, the critical value was found to be $D^* \approx 70$. This value is recovered in the present calculations, when carried out for a sufficiently wide channel, $h = 20$. For lower values of h, however, the critical Damköhler number D^* decreases and for sufficiently narrow channels, the flame appears stable for all values of D. This is clearly seen in Figure 9(a), where $D^* \approx 13$ for $h = 12$ and is below one, and outside the range of the computation, for $h = 8$. Figure 9(b) shows that for lower values of h the flame at the representative value $D = 12$ is always stable.

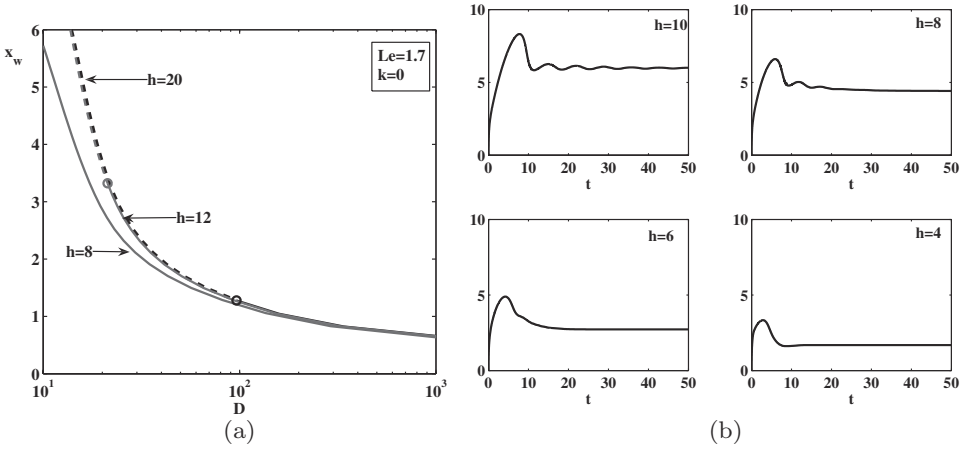

Figure 9. (a) Standoff distance as a function of Damköhler number for edge flames in channels of decreasing width; solid curves identify the stable states and dashed curves the unstable states. (b) Time history of the flame position for $D = 12$ in channels of width $h \leq 5$; in all cases the initial disturbance is damped and the flame regains its steady state position.

3.4. *Differential diffusion*

We now examine the effect of varying the Lewis numbers, retaining $\phi = 1$, for adiabatic conditions. Figure 10 shows a comparison of the edge standoff distance for different values of Le and different channel widths. One sees that the range of Damköhler numbers, or flow rates, for which the edge flame can be stabilized in the channel increases as the Lewis number is decreased. The resulting increase in molecular diffusivity enhances mixing and facilitates stabilization of the premixed edge segment of the flame. Hence, for a lower value of Le the flame can be stabilized in a faster flow. For example, in a channel of width $h = 10$ and for a flow rate corresponding to $D = 2$, the flame is stabilized at a distance $x_w \approx 2$ from the tip of the plate when $Le = 0.8$. For the same flow rate it will be stabilized further away from the plate when Le increases and will be blown off from the channel if $Le = 2$. We also note that differential diffusion is less pronounced in narrow channels. For a channel width $h = 4$, for example, the response curves remain close to each other for a relatively wide range of Lewis numbers.

The variations in Lewis number also have an effect on the overall flame length l_f. Figure 11 shows the dependence of l_f on D in a relatively narrow channel, $h = 4$, for various values of the Lewis number. Due to the increase in molecular mixing that results from the decrease in Le, reactant consumption at the premixed flame segment increases leaving behind significantly less fuel and oxidizer to burn at the trailing diffusion flame. The overall length l_f therefore decreases with decreasing Le.

3.5. *Heat loss*

We now examine the effect of conductive heat loss at the channel walls on the flame structure. The response curves in Figure 12 show a comparison of the flame standoff distance plotted as a function of D for channels of moderate widths, with $k = 10$ and for the adiabatic case $k = 0$. As a result of heat loss the flame standoff distance increases and the range of Damköhler numbers for which the flame can be sustained in the channel is

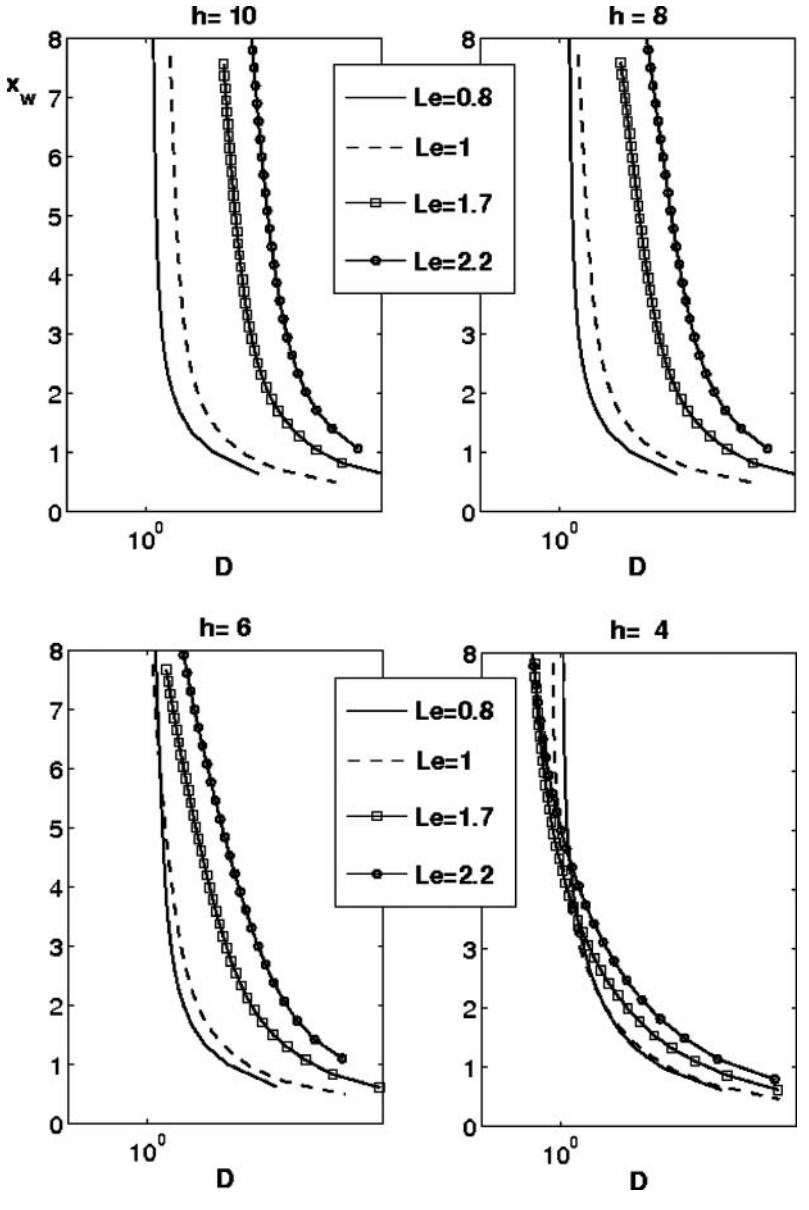

Figure 10. Flame standoff distance as a function of the Damköhler number, for various values of the Lewis numbers and channel widths. Calculated for $k = 0$ and $\phi = 1$.

reduced. We also see that narrow channels are more sensitive to heat losses; for a channel of width $h = 6$ the flame standoff is significantly increased and the range of Damköhler number for which the flame is stabilized is greatly reduced, as a result of heat loss, but there is only a small change between the response curves in the wider channel, $h = 10$.

Figure 13(a) shows response curves for an edge flame stabilized in a very narrow channel, of width $h = 4$, for small heat loss intensities. In such a narrow channel the flame cannot be sustained when the heat loss intensity is as high as $k = 10$, considered in the

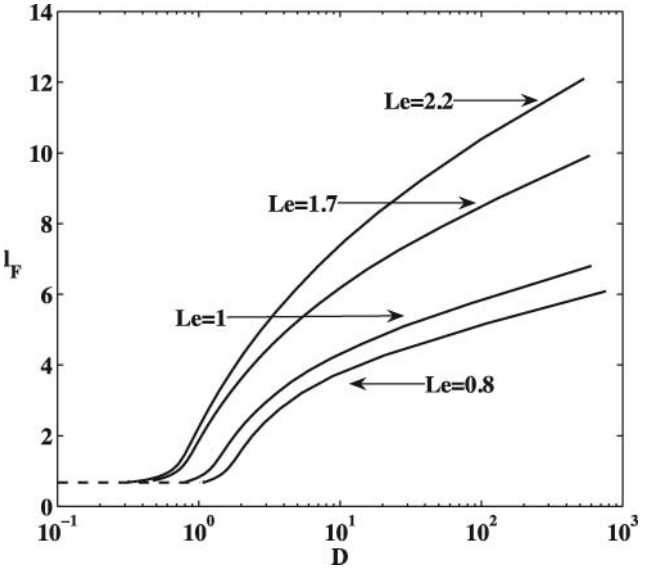

Figure 11. Flame length as a function of Damköhler number, calculated for $h = 4$ for various values of the Lewis number. Calculated for $k = 0$ and $\phi = 1$.

previous figure. The figure shows that for adiabatic conditions the flame is stabilized at $x_w \sim 7.6$ when the Damköhler number $D \sim 0.48$, but is blown off in the presence of a small degree of heat loss. The reduction in burning rate resulting from cooling the mixture in the preheat zone allows the flow to advect the flame farther downstream. As a result, the flame can be more easily blown away from the channel. The figure also shows the vulnerability of the flame to heat losses in narrow channels. For a flow rate corresponding to $D \approx 10$ the flame cannot be sustained in the channel when $k = 0.5$ but is stabilized very close to

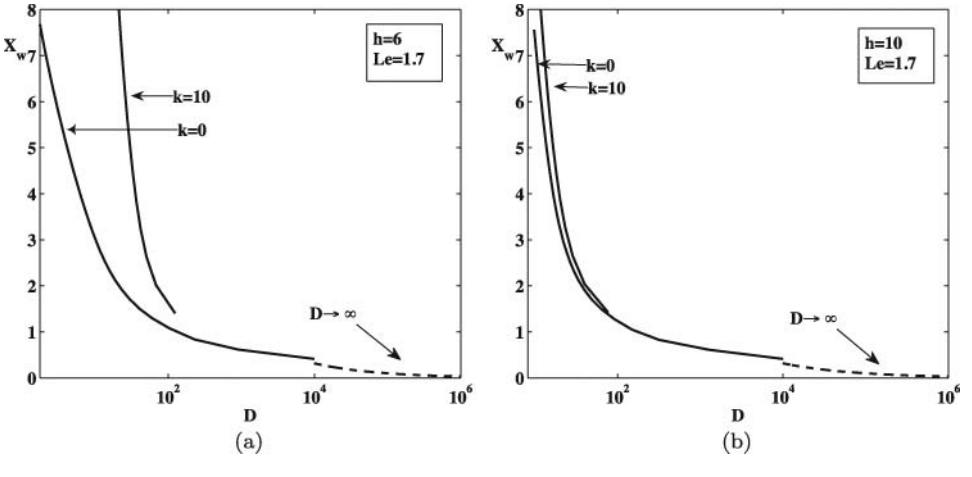

Figure 12. Flame standoff distance as a function of the Damköhler number in channels of various widths, for adiabatic conditions $k = 0$ and in the presence of heat loss $k = 10$. Calculated for $Le = 1.7$ and $\phi = 1$.

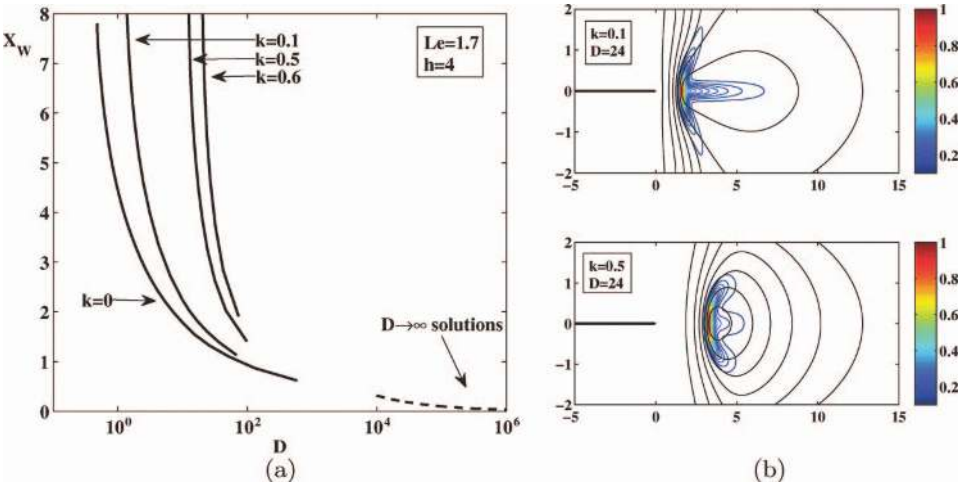

Figure 13. (a) Flame standoff distance as a function of the Damköhler number for edge flames in a very narrow channel of width $h = 4$, in the presence of heat loss, for small increasing values of the heat-loss intensity k. (b) Reaction rate contours (in color) and temperature contours (in black) for two values of the heat loss parameter. Calculated for $Le = 1.7$ and $\phi = 1$.

the tip of the plate (to within two units of length) under adiabatic conditions. Heat losses also have an effect on the flame shape and length, as can be seen in Figure 13(b) where the flame structure is shown for the same flow conditions, $D \sim 24$, and two values of the heat loss parameter. When increasing the degree of heat loss, the length of the trailing diffusion flame is decreased and the reaction is isolated closer to the center of the channel where the temperature is high enough for chemical reaction to occur.

In Figure 14 we show reaction rate contours of flames sustained under different flow conditions in a slightly wider channel, of width $h = 6$, but with $k = 10$ that practically correspond to cold isothermal walls maintained at $\theta \approx 0$. For smaller values of the Damköhler number the flame is pushed far downstream. Since, as a result, more premixing occurs, the flame has a relatively wider leading edge. For larger values of the Damköhler number, the flame is relocated closer to the splitter plate but the reaction is confined to a very narrow region near the center of the channel. The width of the leading edge is now much narrower due to reduction in premixing.

Although under adiabatic conditions the flame in a narrow channel was of finite extent, all the reactants were consumed at the trailing diffusion flame, with no residual fuel and/or oxidizer at the end of the channel. In the presence of heat loss, the reaction freezes where there is a significant drop in temperature, so that residual fuel and/or oxidizer are likely to be found at the end of the channel. Figure 15 shows a comparison of these two cases, i.e., $k = 0$ and 1, in a channel of width $h = 6$ for the same flow conditions. The graph shows fuel mass fraction contours (in color) and profiles of the fuel mass fraction at two locations along the channel. In the absence of heat loss, except for some premixing occurring ahead of the flame, the fuel remains in the upper half, and the oxidizer in the lower half of the channel, burning to completion along the stoichiometric surface $y = 0$. When $k = 1$, however, the excess fuel (or oxidizer) that remains unburned, because of the low temperature near the walls, diffuses into the opposite side from behind the flame. Consequently, residual fuel and oxidizer remain at the end of the channel. At $x = 9.9$, for example, there is fuel along the channel walls on both sides of the axis, as seen in the figure. The small amount present

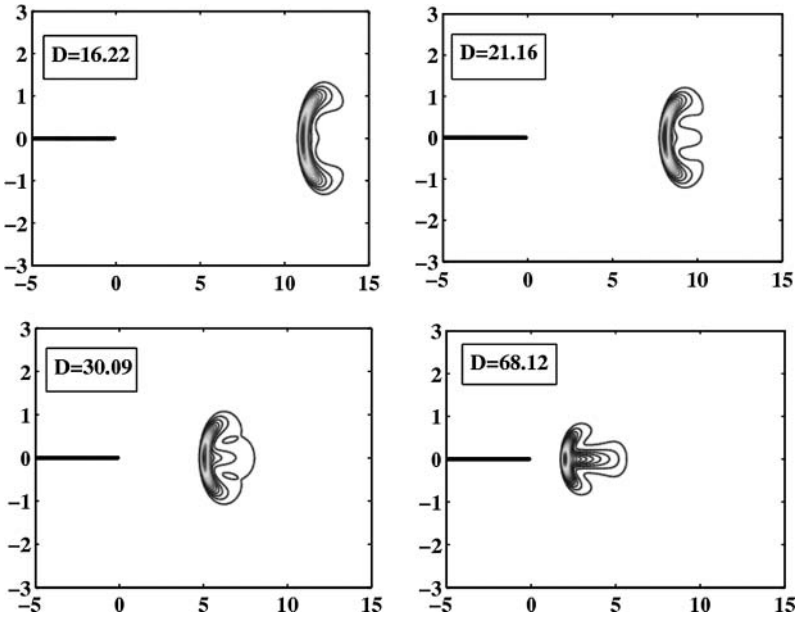

Figure 14. Reaction rate contours for an edge flame in a channel of width $h = 6$ with large heat loss, $k = 10$, for various values of the Damköhler number. Calculated for $Le = 1.7$ and $\phi = 1$.

for $y < 0$ is from the premixing that took place ahead of the leading edge, and convected downstream. At $x = 13.9$, which is well beyond the trailing edge of the flame, fuel is also diffusing into the oxidizer side from behind the flame and there is significant fuel left at the end of the channel. This effect becomes more significant when the channel is slightly wider and the heat loss more excessive. Figure 16 shows reaction rate contours, fuel mass fraction contours, and fuel mass fraction profiles at two locations along the channel for an edge flame in a channel of width $h = 6$ with $k = 10$. In this case the flame is practically reduced to a small "flame cell" and there is significant fuel and oxidizer left unburned at the end of the channel. We note that in the current model there is no mechanics that supports the re-ignition of the unburned mixture; should ignition be possible, however, there would be sufficient fuel and oxidizer available for sustaining a second "flame cell" further downstream much like the experimental observations [11, 13] discussed in the introduction.

Next, we consider the effect of heat losses on the stability of an edge flame in a narrow channel. In unconfined mixing layers spontaneous oscillations resulting from diffusive-thermal effects occur when the Lewis number of one of the two reactants is sufficiently large and D is reduced to below a critical value D^*. For $Le = 1.7$, the critical $D^* = 70$ [22]. It is also known that heat losses promote instabilities, driving spontaneous oscillations even when, in their absence, the flame is stable. Moreover, heat loss could trigger oscillations even when the mixture is diffusive-thermal neutral, i.e., both Lewis numbers equal one [21]. In the adiabatic case we have determined that confinement had a stabilizing effect on the flame and for channels of width below $h = 10$ the edge flame is unconditionally stable. This conclusion, however, changes when heat losses are present. Figure 17 shows the time evolution of the flame position for several values of h and a heat loss parameter, $k = 1$. In the narrower channel, $h = 6$, heat losses promote oscillations for $D = 89.35$, i.e., well above the critical $D^* = 70$ for unconfined flames. In a slightly wider channel, $h = 8$, the

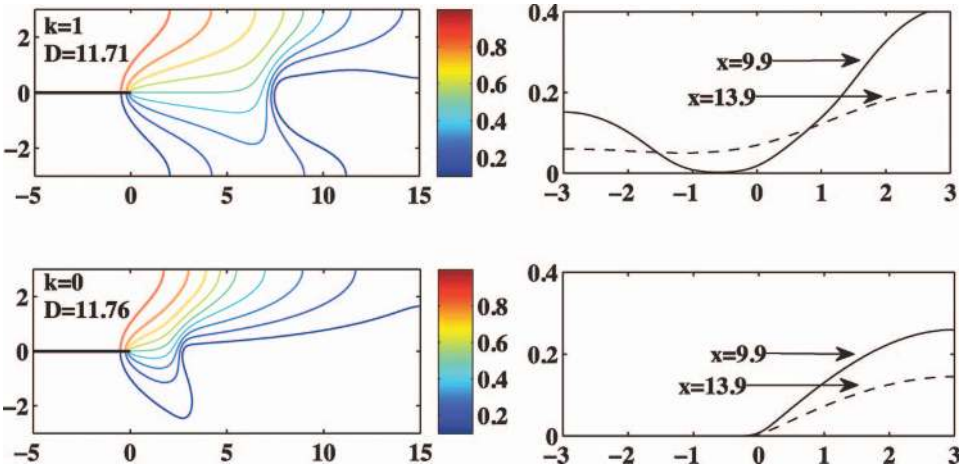

Figure 15. Fuel mass fraction contours for two values of the heat loss parameter (left). Fuel mass fraction across the width of the channel at two locations for two values of the heat loss parameter (right). Calculated for $D \sim 11$, $Le = 1.7$ and $\phi = 1$.

destabilizing effect of heat losses is diminished, and for a channel of width $h = 10$ the flame converges to its steady solution and is stable.

Figure 18 shows reaction rate contours at five distinct times during one period of oscillation. As the flame approaches the splitter plate, the reaction is more intense and the leading edge is highly curved with long premixed wings. Being close to the plate the flame loses heat to the relatively cold plate, the reaction rate diminishes and the edge is pushed downstream by the flow. At a larger standoff distance, the reaction intensity is lower and

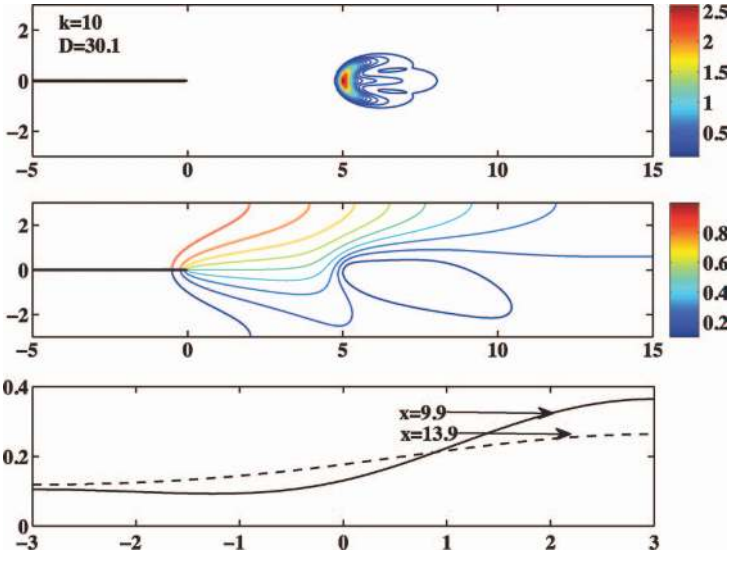

Figure 16. Reaction rate contours (top), fuel mass fraction contours (middle) and fuel mass fraction across the channel at two locations (bottom) for an edge flame in a channel of width $h = 6$ with heat losses $k = 10$. Calculated for $D = 30.1$, $Le = 1.7$ and $\phi = 1$.

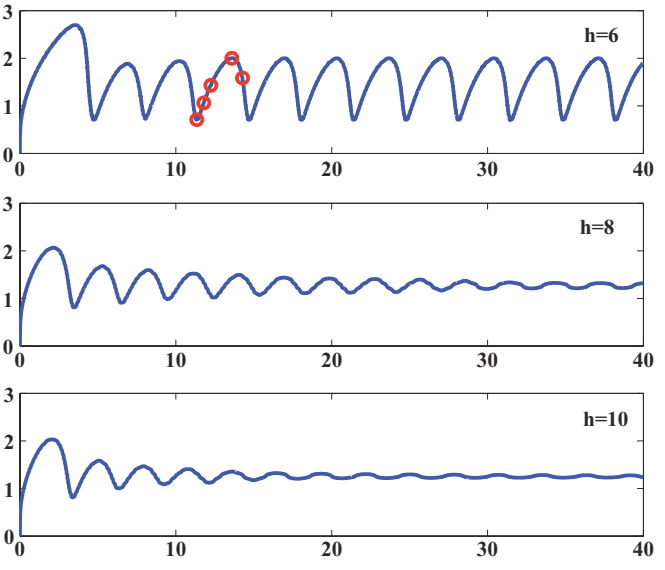

Figure 17. Time evolution of the edge flame position for three values of channel width, in the presence of heat losses with $k = 1$, $D = 100$, and $Le = 1.7$. The points marked on the top plot correspond to the time snapshots, seen in Figure 18.

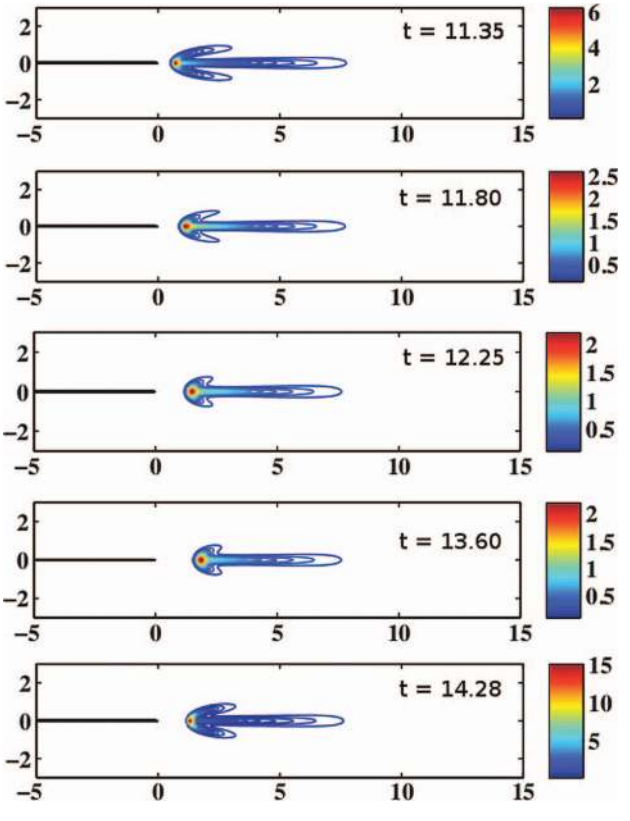

Figure 18. Reaction rate contours for an edge flame in a channel of width $h = 6$ in the presence of heat losses $k = 1$, with $D = 100$, $Le = 1.7$. Each plot corresponds to a snapshot in time.

the wings of the edge flame are significantly shorter. However, it permits more premixing of the reactants ahead of the leading edge which drives the flame back upstream to repeat the cycle. We also notice that the location of the trailing edge remains relatively unchanged and is primarily determined by the extent of heat loss to the channel walls. Hence, it is the leading edge of the flame that oscillates while the trailing diffusion flame remains nearly essentially motionless.

4. Conclusions

The flame in a non-premixed microcombustor has a typical tribrachial structure with its leading edge standing at a well-defined distance from the plate separating the incoming fuel and oxidizer streams. The shape, location, and stability of the edge flame is strongly affected by the confinement and the extent of heat loss to the channel walls. Under adiabatic conditions, a confined flame can be stabilized closer to the splitter plate and sustained for higher values of the flow rate than an unconfined one. In wide channels the flame retains its tribrachial structure, with a trailing diffusion flame aligned along the stoichiometric surface, consuming all the available reactants. In narrow channels, however, the trailing diffusion flame is of finite extent and the premixed edge segment of the flame flattens out, to more closely resemble a premixed flame.

In the presence of conductive heat loss to the channel walls the leading edge of the flame is stabilized farther downstream than under adiabatic conditions, and there is an overall reduction in the length of the trailing diffusion flame. As expected narrower channels are more sensitive to heat losses and the range of flow rates for which the flame can be stabilized in the channel is significantly reduced. Due to heat loss the reaction rate is reduced near the channel walls and for larger values of heat loss the flame is confined to a narrow region in the center of the channel. When heat losses are present, we find residual reactants at the channel end, beyond the flame trailing edge, which indicates that fuel and oxidizer would be available for burning if reignition were possible. We note that the present model assumes that the heat loss coefficient is constant along the wall. Heat conduction along the walls from the flame region towards the colder gas may provide a mechanism for reigniting the residual fuel found downstream. Future work will allow for thermally active walls, which is clearly an important aspect of microscale combustion, and extend the computational domain in order to capture the secondary “flame cells" that have been observed experimentally.

In narrow adiabatic channels the flame is not prone to oscillations, as it is in unconfined mixing layers. Conductive heat losses, on the other hand, which are more significant in narrow channels, promote oscillations. We find oscillations even for fairly large values of the Damköhler number, or sufficiently low flow rates. When flame oscillations are present it is primarily the leading edge which oscillates while the trailing edge remains relatively stable.

Acknowledgments

This work has been partially supported by a NASA GSRP Fellowship (GSRP #7938) and by the National Science Foundation under grant DMS-0708588.

References

[1] J. Daou and M. Matalon, *Flame propagation in Poiseuille flow under adiabatic conditions*, Combust. Flame 124 (2001), pp. 337–349.
[2] J. Daou and M. Matalon, *Influence of conductive heat-losses on the propagation of premixed flames in channels*, Combust. Flame 128 (2002), pp. 321–339.
[3] V. Kurdyumov and E. Fernández-Tarrazo, *Lewis number effect on the propagation of premixed laminar flames in narrow open ducts*, Combust. Flame 128 (2002), pp. 382–394.

[4] C. Cui, M. Matalon, and T.L. Jackson, *Pulsating mode of flame propagation in two-dimensional channels*, AIAA J. 43 (2005), pp. 1284–1292.
[5] P. Ronney, *Analysis of non-adiabatic heat-recirculating combustors*, Combust. Flame 135 (2003), pp. 421–439.
[6] T.T. Leach and C.P. Cadou, *The role of structural heat exchange and heat loss in the design of efficient silicon micro-combustors*, Proc. Combust. Inst. 30 (2005), pp. 2437–2444.
[7] J. Ahn, C. Eastwood, L. Sitzki, and P.D. Ronney, *Gas-phase and catalytic combustion in heat-recirculating burners*, Proc. Combust. Inst. 30 (2005), pp. 2463–2472.
[8] T.T. Leach, C.P. Cadou, and G.S. Jackson, *Effect of structural conduction and heat loss on combustion in micro-channels*, Combust. Theory Model. 10 (2006), pp. 85–103.
[9] Y. Tsuboia, T. Yokomorib, and K. Maruta, *Lower limit of weak flame in a heated channel*, Proc. Combust. Inst. 32 (2009), pp. 3075–3081.
[10] V. Kurdyumov and M. Matalon, *Analysis of an idealized recirculating microcombustor*, Proc. Combust. Inst. 33 (2011), pp. 3275–3284.
[11] C. Miesse, R.I. Masela, M. Short, and M.A. Shannon, *Experimental observations of methane–oxygen diffusion flame structure in a sub-millimeter microburner*, Combust. Theory Model. 9 (2005), pp. 77–92.
[12] C. Miesse, R.I. Masela, M. Short, and M.A. Shannon, *Diffusion flame instabilities in a 0.75 mm non-premixed microburner*, Proc. Combust. Inst. 30 (2005), pp. 2499–2507.
[13] B. Xu and Y. Ju, *Studies on non-premixed flame streets in a mesoscale channel*, Proc. Combust. Inst. 32 (2009), pp. 1375–1382.
[14] S.H. Chung, *Stabilization, propagation and instability of tribrachial triple flames*, Proc. Combust. Inst. 31 (2007), pp. 877–892.
[15] J. Buckmaster, *Edge-flames*, Prog. Energy Combust. Sci. 28 (2002), pp. 435–475.
[16] M. Matalon, *Flame dynamics*, Proc. Combust. Inst. 32 (2009), pp. 57–82.
[17] V.R. Katta and W.M. Roquemore, *Numerical studies on the structure of two-dimensional H_2/air premixed jet flame*, Combust. Flame 102 (1992), pp. 21–40.
[18] I.G. Im and J.H. Chen, *Structure and propagation of triple flames in partially premixed hydrogen–air mixtures*, Combust. Flame 119 (1999), pp. 436–454.
[19] V. Favier and L. Vervisch, *Edge flames and partially premixed combustion in diffusion flame quenching*, Combust. Flame 125 (2001), pp. 788–803.
[20] X. Qin, I.K. Puri, and S.K. Aggarwal, *Characteristics of lifted triple flames stabilized in the near field of a partially premixed axisymmetric jet*, Proc. Combust. Inst. 29 (2002), pp. 1565–1572.
[21] V. Kurdyumov and M. Matalon, *Radiation losses as a driving mechanism for flame oscillations*, Proc. Combust. Inst. 29 (2002), pp. 45–52.
[22] V. Kurdyumov and M. Matalon, *Dynamics of an edge-flame in a mixing layer*, Combust. Flame 139 (2004), pp. 329–339.
[23] V. Kurdyumov and M. Matalon, *Stabilization and onset of oscillation of an edge-flame in the near-wake of a fuel injector*, Proc. Combust. Inst. 31 (2007), pp. 909–917.
[24] V. Kurdyumov and M. Matalon, *The porous-plug burner: Flame stabilization, onset of oscillation, and restabilization*, Combust. Flame 153 (2008), pp. 105–118.
[25] J.A. Bieri, V. Kurdyumov, and M. Matalon, *The effect of thermal expansion on edge flames stabilized in narrow channels*, Proc. Combust. Inst. 33 (2011), pp. 1227–1234.
[26] C.K. Law, *Combustion at a crossroads: Status and prospects*, Proc. Combust. Inst. 31 (2007), pp. 1–29.
[27] F.A. Williams, *Combustion Theory*, Benjamin/Cummings, Menlo Park, CA,1985.
[28] Y. Ju and C.W. Choi, *An analysis of sub-limit flame dynamics using opposite propagating flames in mesoscale channels*, Combust. Flame 133 (2003), pp. 483–493.
[29] Y. Ju and C.W. Choi, *Theoretical and experimental studies on mesoscale flame propagation and extinction*, Proc. Combust. Inst. 30 (2005), pp. 2445–2453.